

PERFORMANCE OF A TRANSMUTATION ADVANCED DEVICE FOR SUSTAINABLE ENERGY APPLICATION

C. García¹, A. Pérez-Navarro², A. Escrivá², A. Abánades³,
Rosales J.¹, L. García¹

- (1) Instituto Superior de Tecnologías y Ciencias Aplicadas (INTEC), Avenida Salvador Allende y Luaces, Quinta de Los Molinos, Plaza, La, Habana, Cuba
- (2) Instituto de Ingeniería Energética, Universidad Politécnica de Valencia, Valencia 46022, España.
- (3) Grupo de Modelización de Sistemas Termoenergéticos, Universidad Politécnica de Madrid, c/Ramiro de Maeztu 7, 28040 Madrid, España

Abstract

Preliminary studies have been performed to design a device for nuclear waste transmutation and hydrogen generation based on a gas cooled pebble bed accelerator driven system, TADSEA (transmutation advanced device for sustainable energy application). In previous studies we have addressed the viability of an ADS Transmutation device that uses as fuel wastes from the existing LWR power plants, encapsulated in graphite in the form of pebble beds, being cooled by helium which enables high temperatures, in the order of 1200 K, to facilitate hydrogen generation from water either by high temperature electrolysis or by thermo chemical cycles. To design this device several configurations were studied, including several reflectors thickness, to achieve the desired parameters, the transmutation of nuclear waste and the production of 100 MW. of thermal power. In this paper we are presenting new studies performed on deep burn in-core fuel management strategy for LWR waste. We analyze the fuel cycle on TADSEA device based on driver and transmutation fuel that were proposed for the General Atomic design of a gas turbine-modular helium reactor. We compare the transmutation results of the three fuel management strategies, using driven and transmutation, and standard LWR spend fuel, and present several parameters that describe the neutron performance of TADSEA nuclear core as the fuel and moderator temperature reactivity coefficients and transmutation chain.

1 INTRODUCTION

Nuclear Energy sustainability will depend on the actual capability of reducing both the inventory and long-term radio-toxicity of nuclear waste of present fission reactors, mainly dominated by the amount of transuranic isotopes remaining on the spent fuel. The IV Nuclear Energy Reactors Generation and the Accelerator Driven Systems (**ADS**) are the two main options to achieve this goal. Preliminary studies have been made to design a device for simultaneous transmutation of nuclear waste and hydrogen generation, based on a ADS that uses the fuel containing the wastes from the existing LWR power plants, encapsulated in graphite, in the form of pebble beds, cooled by helium, [**García et al, 2009**], called **TADSEA**, (Transmutation Advanced Device for Sustainable Energy Application) which enables high temperatures, in the order of 1200 K and 100 Mw of thermal power, to facilitate hydrogen generation either by high temperature electrolysis or by thermochemical cycles. Previously, in [**Abánades et al, 2006**], several studies were made to get an engineered design of Pebble-Bed Transmuter (**PBT**), that contributed for the TADSEA design. Similarly, PBT is a gas-cooled subcritical nuclear core, filled with graphite-fuel pebbles and driven by a cyclotron accelerator. PBT uses the well known TRISO fuel [**Venneri et al, 2001**]. It can work based on the deep burn concept and the initial fuel loaded in PBT includes plutonium and minor actinides isotopes in a proportion similar to that existing in the typical spent fuel from a LWR power plant with a burnup of 40 MWd/kg and after 15 years of radioactive cooling in the plant pools. [**A European Roadmap for Developing Accelerator Driven Systems (ADS) for Nuclear Waste Incineration, 2001**].

In this paper new studies about deep burn strategies of spent fuel from LWR on TADSEA and PBT are presented. Here we have analyzed the behavior in PBT of the spent fuel management strategy, proposed by [**Talamo et al, 2004, Rodríguez, 2003**] for the so called Deep Burn Modular Helium Reactor (**DB-MHR**). We compared three strategies for fuel management: first of all, the traditional one, named “spent fuel” (**SF**) that uses spent fuel from LWR. Second, the one in which the transuranic elements are divided in two groups, a “driven fuel” (**DF**) composed only by Plutonium isotopes and Np^{237} is used in PBT core like SF, and third, the fuel management strategy in which after the DF has reached the stationary state we feed PBT core with a layer of “transmutation fuel”, composed by Am^{241} , Am^{243} y Cm^{244} isotopes from spent DF and it is mixed after discharge from the reactor core with the Am and Cm isotopes, which was set-aside after UREX.

We compared mass depletion of Plutonium isotope and Minor Actinides (**MA**) after an irradiation of 990 days in the system, and the time evolution of radio-toxicity for the initial load and the unload fuel of the three strategies of fuel irradiation.

For a better understanding of the transmutation process we built the transmutation chain for TF, obtained by MNCPX code. It describes how the isotopic changes of main transuranic isotope occur. We also show parameters describing the neutronic behavior of TADSEA, such as the fuel and moderator temperature reactivity coefficients.

2 Main PBT and TADSEA characteristics.

2.1 PBT characteristics

PBT is a subcritical system cooled by helium and moderated with graphite that uses as fuel small amounts of transuranics elements diluted in the form of TRISO particles in a graphite matrix, as to form a pebble bed configuration as displayed at figure 1. The system is maintained by a proton accelerator with beam energy in the order of 380 MeV and intensities close to 10 mA. The spallation target that allocates a eutectic lead-bismuth in molten state uses a new geometrical design in a conical form to alleviate stress in the window and increase the neutron source size. Core of the assembly is formed by a cylinder containing the pebbles and, in its center, the spallation target. Fuel is confined in 3 cm radius pebbles, with an external layer of 5 mm thickness in pyrolytic graphite and the remaining sphere of 2.5 cm filled up with TRISO particles of 1 mm diameter containing the fuel in a structure that includes an external isotropic pyrolytic graphite layer, a SiC barrier, an inner isotropic pyrolytic graphite layer and, in the center, a buffer composed by a porous pyrolytic graphite. Main advantage of a pebble bed core is the possibility for a continuous core recharge without plant operation interruption. Besides, the porous material in the TRISO particles facilitates the storage of big quantities of fission products and enables the system to reach higher burnups, in the order of 740 MWd/Kg [C. Rodríguez, A Baxter, 2003] and can afford temperature of 1600°C. In a repository environment, spent TRISO particles should maintain their integrity for millions of years, even if they would permanently be flooded with groundwater.

PBT core is composed by 20 layers of pebbles disposed in a honeycomb way (hexagonal lattice), the pebbles stand over the holes of the layer immediately below, the packing factor is in the order of 0.74 and thermal power is of 10 MW in the stationary state.

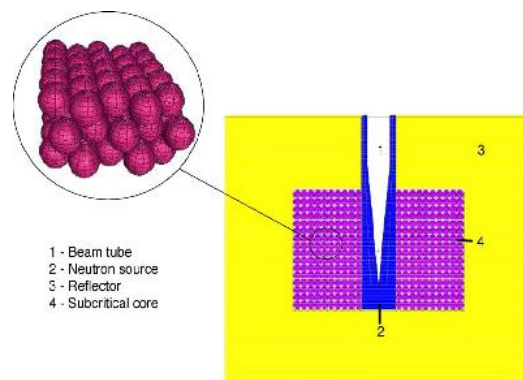


Figure 1: PBT configuration

2.2 TADSEA characteristics.

For application to hydrogen generation, given the big amounts of this energy vector to be required in a future energy scenario, was important to increase as much as possible the TADSEA thermal power looking for values in the order of 100 MW. With this goal, the proton beam characteristics have been increased up to the limits expected in the technical development of accelerators in the near future: 1 GeV and 10 mA. Besides, increasing the geometrical dimensions and maintaining the maximum power density in a value, 7 W/cm³, acceptable from a technical point of view is also possible to increase power, but with the constraint of keeping the transmutation capabilities of the system and no deterioration of the power profiles.

To guarantee the safety of the device, a study of the dependence of the multiplication factor on the reflector thickness was addressed. Results indicated that for the most extreme condition, reflector radial thickness below 70 cm guarantee Keff always below 0.95. Table 1 summarises the main parameters for both, PBT and TADSEA devices.

Table 1: Main parameters of PBT and TADSEA

Parameter	Value		Units
Thermal Power	10	100	Mw
Accelerator Power	3.8	10	Mw
Protom beam energy	380	1000	Mev
Protom beam intensity	10	10	mA
Fuel	Balls with graphite + TRUs	Balls with graphite + TRUs	-
Fuel mass (Pu+MA)	14.64	124.5	Kg
Core volume	1.69	14.38	m ³
Number of balls	11064	94092	
Average power density	6	7	W/cm ³
Keff	0.84	0.94	-

2.3 Neutronics calculations

For simulation purposes, the PBT and TADSEA cores were divided in 10 horizontal layers that were considered in the calculations as homogeneous zones. The PBT and TADSEA neutronics was calculated with MCNPX 2.6e.

The MCNPX 2.6e code [Gregg McKinney et al, 2007] has been chosen to simulate the neutronics behavior, because this new version incorporates a set of capabilities to facilitate the simulation of ADS transmutation systems, such as the LAHET code [Prael et al,1989]

that allows for the calculation of the neutron chain generated by a proton beam and its transport at high energies, making possible to simulate in a single run the transport of protons and neutrons in the spallation target and the incorporation of the neutrons, as a fast neutrons source, to the core of the subcritical assembly containing the fuel based on the nuclear wastes.

The new version also incorporates the CINDER90 and the MonteBurns codes that facilitate the calculation of the isotopes evolution in the core. Currently, the MCNPX possibility to calculate the fuel burnup and the variation in the isotope composition are limited to critical configurations, so, in our simulations we calculate the burnup in the subcritical core by considering an average neutron flux in each zone condensed to a single speed and spatially averaging for the flux distribution deduced from the eigenvalues problem analysis. CINDER90 works with 63 energy groups and the transversal cross sections for these 63 groups are condensed by using a generic spectrum. This approach can produce some discrepancies in the final inventory for the isotopes generated from the fission products. Nevertheless, for comparison of different configurations this limitation does not introduce significant errors, as was demonstrated before. [García et al, 2009].

Another MCNPX.2.6e new capability used for this study is the incorporation of the predictor-corrector technique for the burnup calculation. This technique allows for a use of longer time step without significant precision loss in the results.

3 Spent fuel management strategies for PBT and TADSEA.

Preliminary studies have shown that the isotopic depletion of nuclear fuel under deep burn concept in PBT and TADSEA subcritical cores has a similar behaviour. Therefore, we decided to compare three different spent fuel management strategies, called “spent fuel” (SF), “driven fuel” (DF) and $DF + SF$, and to model the burnup using the PBT core as it demands a lower computational cost due to its smaller size.

3.1 Fuel shuffling strategies

The Deep Burn concept is based on the use of Driven Fuel, rich in fissile actinides (Pu^{239}) and Transmutation Fuel, rich in non-fissile actinides. The DF provides the excess reactivity to drive the power production and sustain large effective transmutation rates. The TF provides burnable poison and reactivity control. The LWRs waste is reprocessed by uranium and fission products extraction (UREX). The final products of the LWRs spent fuel reprocessing are NpPuO1.7 and AmCmO1.7; the first material constitutes the Driven Fuel (DF) [Talamo et al, 2004]. The DF is the primary nuclear fuel for the TADSEA or PBT and it sustains the fission chain reaction, mainly by Pu^{239} . AmCmO1.7 from spent DF is mixed after discharge from the reactor core with the AmCmO1.7, which was set-aside after

UREX, to build fresh Transmutation Fuel (TF). After irradiation, spent TF is sent into the repository.

The main objective of the DF concept has been the extended destruction of Pu²³⁹, one of the major contributors to long lasting radiotoxicity and the major proliferation concern. We have also focused our attention on the transmutation of Minor Actinides because of their radiological importance, and we tried to get their transmutation process with the TF burning. PBT operation procedure assumed for the simulation includes an initial step where each level is filled with fresh fuel. And in cycles of 99 days, each layer is moved to a lower level, introducing new fuel in the top layer and extracting the balls from the bottom one. With this scheme, the fuel is burned up during 990 days and, after 10 cycles; the system reaches composition equilibrium, where there is only fresh fuel in the first layer while for the last one the fuel has passed a complete 99 days cycle for each of the previous layers. We simulated three spent fuel management strategies in PBT core. SF strategy feed with fresh fuel from typical spent fuel from a LWR. DF fuel shuffling strategy is like than SF.

When DF reached the equilibrium stage, (here we considered 20 cycles) we feed a layer with fresh TF, after we continued feeding with DF layers. The TF layer crosses the PBT core during 10 cycles, and after is extracted as irradiation fuel and sent into repository. The TF layer loaded contains the mass of AmCmO1.7, which was set-aside after UREX and has been belong to 9 remaining DF layers, plus the mass of AmCmO1.7 belonging to irradiated 9 layer of DF, that were 990 days in PBT core. The irradiated DF was reprocessed in a second step.

3.2 Evolution of isotopic composition for studied spent fuel management strategies

Tables 2 and 3 show the mass load and unload of PBT for SF and DF strategies. Third row gives the variation in % of initial mass relative to final mass according to following expression:

$$\Delta\rho^j = \left\{ \frac{\rho_{initial}^j - \rho_{final}^j}{\rho_{initial}^j} \right\} * 100$$

Where $\Delta\rho^j$ is the variation of mass of isotope j with burnup. $\rho_{initial}^j$ is the initial or final mass of isotope j.

The precedent sign plus means decrease and precedent sign minus means increase.

In Table 3, the value of variation of mass of Am²⁴¹, Am²⁴³ y Cm²⁴⁴ in % are in relation to the mass which was set-aside after UREX process when were building fresh DF, because the initial mass of these isotope in DF are zero.

Table 2: Initial and final composition of SF in PBT core

Mass (g)	Np ²³⁷	Am ²⁴¹	Cm ²⁴²	Am ²⁴³	Cm ²⁴⁴	Pu ²³⁸	Pu ²³⁹	Pu ²⁴⁰	Pu ²⁴¹	Pu ²⁴²
Initial	655	752	0	134	24	203.1	7512	3482	1165	713
Final	251.1	41.2	78.2	485.8	427.2	635.8	117.6	364.8	409.3	1742
% Depletion	+61.6	+94.4	-	-262.5	-1680	-213	+98.4	+89.5	64.9	-144.3

Table 3: Initial and final composition of DF in PBT core

Mass (g)	Np ²³⁷	Am ²⁴¹	Cm ²⁴²	Am ²⁴³	Cm ²⁴⁴	Pu ²³⁸	Pu ²³⁹	Pu ²⁴⁰	Pu ²⁴¹	Pu ²⁴²
Initial	759.1	0	0	0	0	223	8469	3423	1251	759.1
Final	363.3	61.5	45.7	204.8	236	439.9	208.7	749.4	948.8	1667.0
% Depletion	+52.1	-6.3	-	-213.9	-593	-97.5	+97.5	+78.1	+24.2	-119.6

We can observe in DF that mass of Cm²⁴², Am²⁴³ y Cm²⁴⁴ increase, nevertheless they grow less in relation to the mass which was set-aside after UREX process than the same isotopes in SF. Am²⁴¹ in DF grow softly, it is logical because it is absent in initial load. In figure 3 (b) we can see that mass of Am²⁴¹ reach a peak and after begin to decreases. In SF, where Am²⁴¹ has a big initial mass, it decreases considerably with burnup.

In both case, SF and DF, the mass of Pu²³⁹ and Pu²⁴⁰ afford a great depletion, it is the main goal of deep burn concept, while Np²³⁷ and Pu²⁴¹ decrease their mass too, but Pu²⁴¹ less in DF. The Pu²³⁸ mass grow considerably more in SF than DF, and Pu²⁴² mass grow softly less in DF. (See fig. 2 (a) and (b)).

The whole mass of Plutonium isotopes decrease with burning for DF in 72%, while SF achieves 75%. The difference is because DF is formed fundamentally by Plutonium and to obtain the same burnup need a longer cycle. The Plutonium has a similar behavior with burnup for both spent fuel management strategies.

The whole depletion of MA with burnup (Np, Am and Cm) is an 18% rate decreasing for SF and a 16% rate increasing for DF, considering the mass which was set-aside after UREX process. The last take place because DF are not formed by Am²⁴¹. This isotope has a great depletion with burnup for SF, Am²⁴¹ become to Cm²⁴² by successive neutronics capture and beta disintegration. Due to there are not Am²⁴¹ for initial composition of DF, then Pu²³⁸ increase less than for SF.

When the stationary stage is reached for DF strategy we began a new fuel cycle, we feed PBT core with a fresh TF layer, after we continued feeding with DF layers. The spent fuel

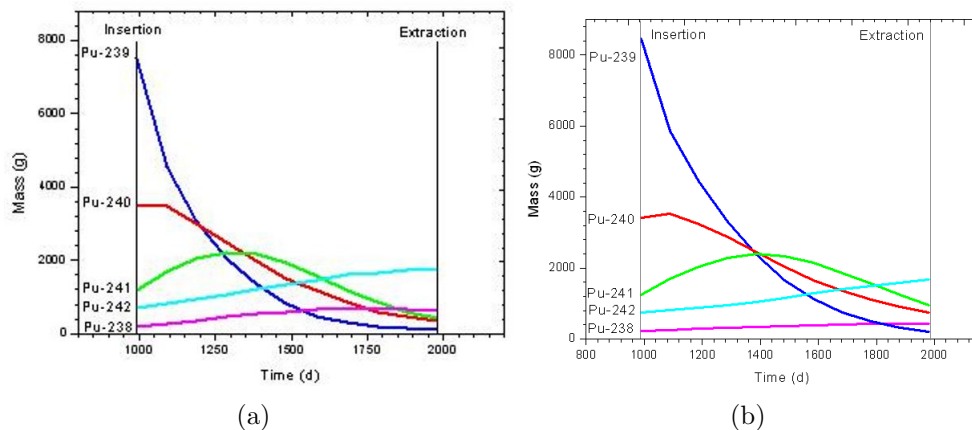


Figure 2: Results for the evolution of Pu isotopes in PBT (a) SF, (b) DF

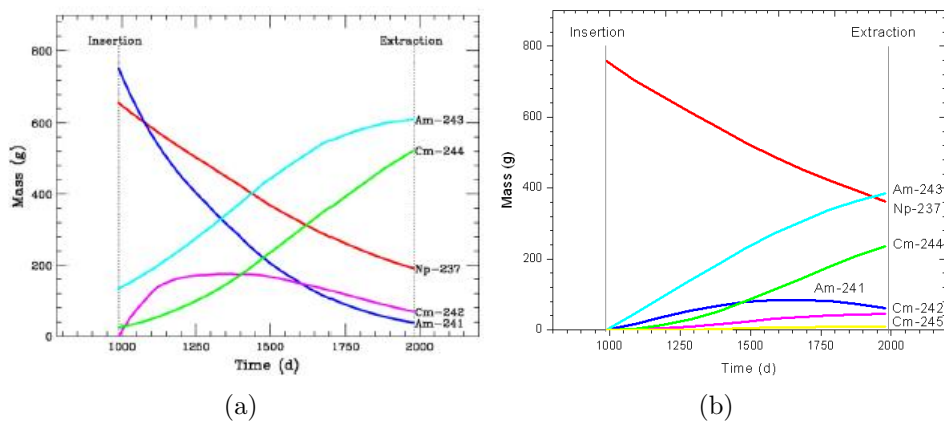


Figure 3: Results for the evolution of MA isotopes in PBT (a) SF, (b) DF

Table 4: Initial and final composition of TF in PBT core

	Np ²³⁷	Am ²⁴¹	Cm ²⁴²	Am ²⁴³	Cm ²⁴⁴	Pu ²³⁸	Pu ²³⁹	Pu ²⁴⁰	Pu ²⁴¹	Pu ²⁴²
IM (g)	0.0	1050	0.0	563.8	275.9	0.0	0.0	0.0	0.0	0.0
FM (g)	0.8	36.5	71	188.2	545.2	428.3	61.5	46	22.2	119.7
% Var	0.04(*)	+96.5	3.7(*)	+66.6	-97.6	22.7(*)	3.3(*)	2.4(*)	1.2(*)	6.3(*)

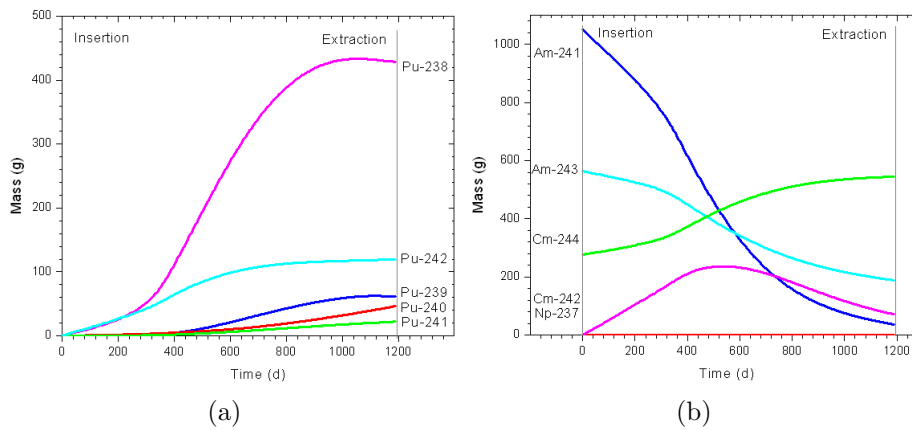


Figure 4: Results for the evolution of Pu (a) and MA (b) isotopes in TF layers of PBT

management strategy where we use one layer of TF and 9 layers of DF was called *DF + TF* strategy. Here layer of TF crosses PBT core in 99 days cycles. Figures 4 (a) and 4(b) show the time variation of the mass for the different plutonium isotopes and the minor actinides, respectively, for the layer of TF crossing the PBT core. Table 4 gives the initial and final mass of MA and isotopes of Plutonium for 990 days of burning of TF layer. The variation in % is referred to initial mass of MA only. In table 5 we can see initial and final mass of transuranic for *DF + TF* strategy. ¹

In table 4 we can observe that among the Plutonium isotopes, only Pu²³⁸ has a significant buildup in TF layer. It reaches a stationary concentration because the process of appearing (Cm²⁴² disintegration) and disappearing (neutronics capture) reach equilibrium. In *DF+TF* strategy (table 5), we can see that initial mass of Pu²³⁸ increases 289%, it is higher than for SF (213%). Nevertheless Am²⁴³ mass decreases significantly, while in SF enlarge. The Am²⁴¹ mass decrease a 96.5% in *DF + TF* strategy, while decrease a 94.5% for SF. The Cm²⁴⁴ mass increases too for *DF + TF* strategy but increase less than for SF, 96.7%

¹(*) The variation in % is referred to initial mass of MA.

Table 5: Initial and final composition of $DF + TF$ in PBT core

	Np ²³⁷	Am ²⁴¹	Cm ²⁴²	Am ²⁴³	Cm ²⁴⁴	Pu ²³⁸	Pu ²³⁹	Pu ²⁴⁰	Pu ²⁴¹	Pu ²⁴²
IM (g)	759.1	1050	0.0	563.8	275.9	223	8469	3423	1251	759.1
FM (g)	364.1	36.5	116.7	188.2	545.2	868.2	270.2	795.4	971	1786.7
% Var	+52	+96.5	-	+66.6	-97.6	-289.3	96.8	+76.8	22.4	-135.4

and 1680% respectively. The last behavior mainly occurs caused by the Cm²⁴⁴, which came from quickly disintegration of Am²⁴⁴, accumulate more for SF, because here there are more Am²⁴³. (see fig. 3 (a)).

Summarizing, $DF + TF$ strategy obtained in comparison with SF strategy, a significantly decrease of initial mass of Am²⁴³, more decrease in the Am²⁴¹ mass, less rise of Cm²⁴⁴, and an build-up of Pu²³⁸, it also maintains the same reduction in Np²³⁷ and the rest of Plutonium isotopes, except Pu²⁴¹.

3.3 Transmutation Chain.

We calculated the capture and fission cross section for one velocity of transuranic elements that they form the Transmutation Fuel and we built transmutation chain for it. The transmutation chain shows the relative probabilities of disintegration, capture and fission of each isotope of chain; it allows explaining their transmutation probability in specific operation PBT conditions.

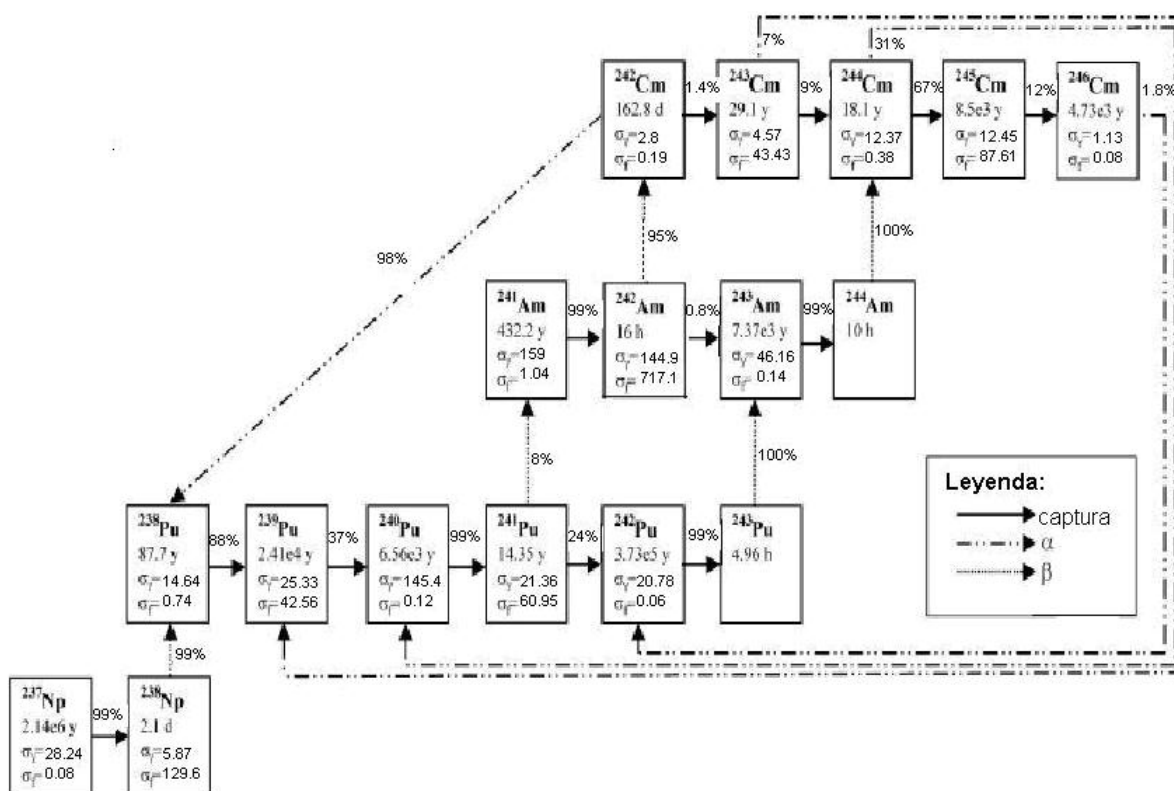
Cross sections were calculated for the end of each cycle of 99 days, for each interesting transuranic isotope in all layers for those that the TF traffics inside PBT core. In all case we obtained similar result and for this reason we only show the values for the end of first cycle. Figure 5 presents the transmutation chain for burning TF, for the end of first cycle, or first layer at 99 days of burning. Result was compared with those obtained by [Talamo et al, 2004] and we observed a very good agreement.

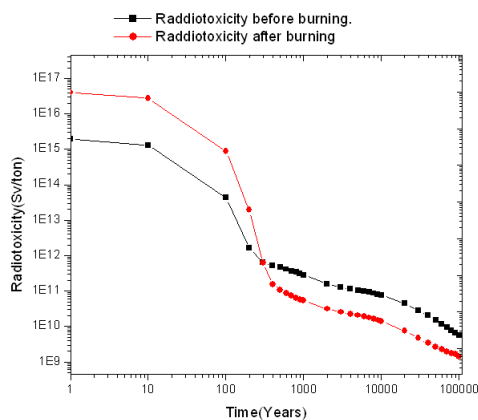
3.4 Time evolution of radiotoxicity for studies spent fuel management strategies.

The radiotoxicity of a nuclide is determined by the product of the activity and the effective dose coefficient e for a given isotope $Radiotoxicity = Activity * e$

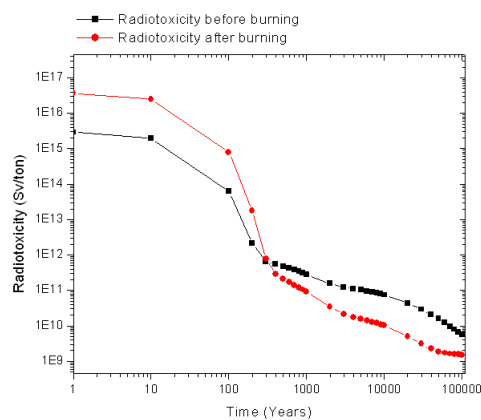
The activity is just the number of disintegrations per second and is measured in units of Becquerel, Bq (1 Bq = 1 disintegration per second). The effective dose coefficient e is a measure

Figure 5: TF transmutation chain. The second row of the boxes reports the half-life constant. The third and fourth rows report the one group effective cross sections for the neutron capture and fission calculated at the end of de first cycle of TF. The percentages are the relative reaction rates and sum up to 100% with fission probability and negligible reaction channels.

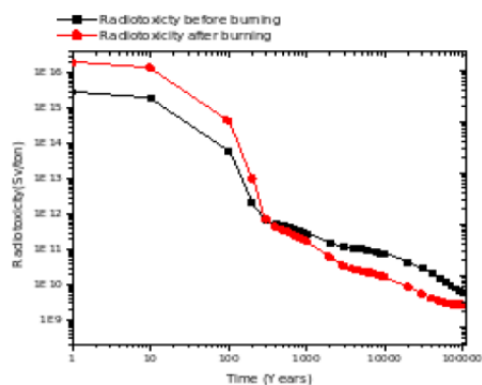




(a) Time evolution of radiotoxicity for SF.



(b) Time evolution of radiotoxicity for $DF + TF$.



(c) Time evolution of radiotoxicity for DF.

Figure 6: Time evolution of radiotoxicity for SF (a), $DF + TF$ (b) and DF (c)

of the damage done by ionising radiation associated with the radioactivity of an isotope. It accounts for radiation and tissue weighting factors, metabolic and biokinetic information. It is measured in units of Sievert per Becquerel (Sv/Bq) where the Sievert is a measure of the dose arising from the ionisation energy absorbed. [A European Roadmap for Developing Accelerator Driven Systems (ADS) for Nuclear Waste Incineration, 2001].

In calculating radiotoxicity, normalized to the initial mass of the fuel loaded in the device, we have taken into account both the initial isotopes and those with significant lifetimes generated along the cycle.

In the figures 6 (a), 6 (b) and 6 (c) is showed the time evolution radiotoxicity by inhalation for both: the charge and the discharge of system for studies spent fuel management strategies SF, DF+TF and DF respectively. We considered in DF the contribution to radiotoxicity for

both of Am and Cm which was set-aside after UREX process.

In Fig. 6 (a) we can observe during the first 300 years there is a relative increase in the discharge radiotoxicity in relation to load. The last is possible because Cm²⁴⁴ appeared with fuel burning process and it has a $T_{1/2}$ equal to 18 years and it contributes meaningfully to radiotoxicity in this period. But after this time the tendency reverts and an order of magnitude decrease is obtained for the discharge radiotoxicity in relation to the initial load one. For example, for 1000 years we obtained for SF ($3.06 \cdot 10^{11}$ to load, and $5.84 \cdot 10^{10}$ Sv/Ton, to unload).

In Figure 6 (b) ($DF + TF$) we can see the same than for SF during the first 300 years. And here the tendency reverts too before this time. For more long time, before 1000 years the main contributions to radiotoxicity to load are in Am²⁴¹, by its great values of activity and Pu²⁴⁰ by its big mass and great activity. The radiotoxicity values of both are an order of magnitude higher than remaining isotopes.

The time evolution radiotoxicity has a similar behavior for SF and $DF + TF$ after 1000 years, although is slightly less for $DF + TF$. For example for 5000 years for SF and $DF + TF$ the radiotoxicity values to load are $1.06 \cdot 10^{11}$ Sv/ton, and $1.02 \cdot 10^{11}$ Sv/ton respectively, and to unload are $2.07 \cdot 10^{10}$ Sv/ton and $1.53 \cdot 10^{10}$ Sv/ton, 35% less for $DF + TF$ to unload. In this time the main contributions to radiotoxicity to load are the Pu²³⁹ and Pu²⁴⁰ and to unload the Pu²⁴⁰.

For more long time, the radiotoxicity to unload for $DF + TF$ will be always less than SF, For example, at 10 thousand years for $DF + TF$ radiotoxicity is $1.01 \cdot 10^{10}$ Sv/ton and for SF is $1.42 \cdot 10^{10}$ Sv/ton (40% less).

Radiotoxicity to load for DF (**Fig. 6 (c)**) has a similar behavior to the SF, and to unload it shows a light increase for time after 300 years in relation to SF and $DF + TF$.

After 300 years, spent fuel management strategy called $DF + TF$ leads to a considerable decrease of time evolution radiotoxicity in relation to the initial load one. This decreasing is stronger than for SF strategy in a 30 to 40%. But if we take account the poor energetic contribution of TF layer and it need a second step in reprocessing process, is necessary to make a careful evaluation of the alternative of burning MA in a fast system with full recycle, and using the spent fuel management strategy called DF to obtain the main goal, the extended destruction of Pu²³⁹.

4 Reactivity temperature coefficients.

We calculated the temperature coefficients for a temperature excursion affecting only the cross-sections either of the fuel or of the moderator. Here we focused our studies at the beginning of first cycle at PBT for DF composition. We considered that graphite of inside pebbled matrix and metal fuel formed by Np²³⁷ and Plutonium isotopes were at the same temperature. We used the available library in XSDIR, ENDL/B VI.2 [LA-CP-05-0369, 2005]. We ran one thousand cycles and one thousand histories per cycle for eigenvalues

Table 6: Fuel Temperature Reactivity Coefficients (FTRC)

Temperature range (K)	K_{eff}^1	Std desv.	K_{eff}^2	Std desv.	FTRC pcm/K	
293.6 - 600	0.90417	0.00051	0.89588	0.000888	-3.34	± 0.56
600 - 800	0.89588	0.00088	0.88800	0.00089	-4.95	± 1.11
800 - 1200	0.88800	0.00089	0.88240	0.00085	-1.79	± 0.55

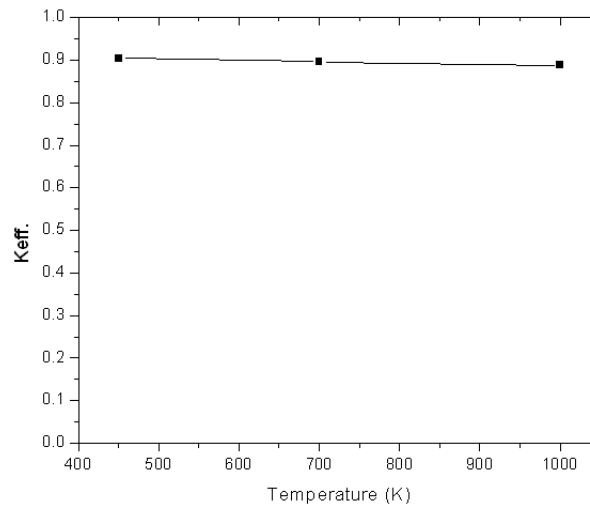


Figure 7: K_{eff} as function of fuel temperature in PBT, beginning of first cycle.

calculations.

Table 6 gives eigenvalues calculated for each fuel extreme temperature in the considered ranges and standard deviations too and the Fuel Temperature Reactivity Coefficients (**FTRC**), calculated by following expression:

$$FTRC = \frac{\rho^{T_2} - \rho^{T_1}}{T_2 - T_1} = \frac{\frac{1}{K_{eff}^{T_1}} - \frac{1}{K_{eff}^{T_2}}}{T_2 - T_1}$$

Where $K_{eff}^{T_1}$ and $K_{eff}^{T_2}$ are the eigenvalues at temperature T_1 y T_2 respectively.

We obtained similar values to those reported by [Zakova and Talamo, 2008] for Plutonium fuel. Figure 7 shows the dependence of eigenvalue K_{eff} of fuel temperature. We can observe that K_{eff} decrease with temperature leading to a negative fuel temperature feedback. Increasing the graphite temperature causes a shift to higher energies of the *Maxwellian* part of the neutron spectrum; this phenomenon drives the moderator temperature reactivity coefficient, especially when we have fuel with plutonium.

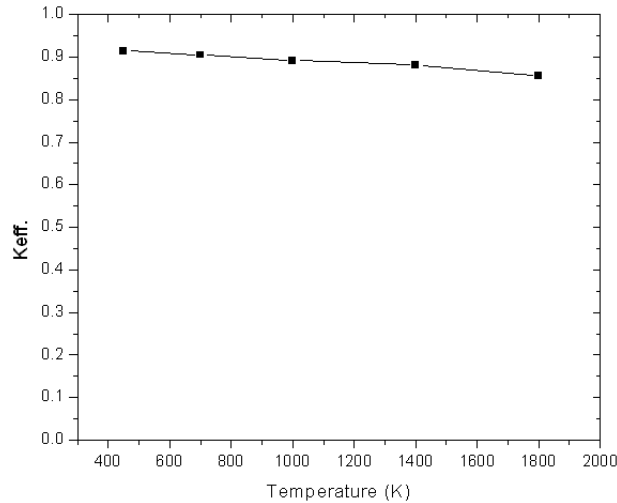


Figure 8: K_{eff} as function of moderator temperature in PBT, beginning of first cycle.

Table 7 shows the values of Moderator Temperature Reactivity Coefficients (**MTRC**) for several temperature ranges. We considered the same temperature at inside and outside graphite pebbled. For graphite of reflector, always we considered 300 K of temperature. The lattice nuclei bindings are taken into account by the scattering function, $S(\alpha, \beta)$ of graphite, available in the ENDL/B V nuclear data library at 300, 600, 800, 1200, 1600 and 2000 K.

The MTRC values were calculated by similar expression that was used for FTRC. The values of MTRC calculated by us for DF in PBT system have a good agreement with those reported by [**Zakova and Talamo, 2008**] for plutonium fuel.

The Fig.8 shows the K_{eff} dependence in PBT as function of the moderator temperature. We obtain a relatively more flat behavior of K_{eff} as function temperature than one reported for the advanced high-temperature reactor (AHTR) proposed by the Oak Ridge National Laboratory, although we can watch too here that K_{eff} curve undergoes a change of slope after 1200 K, because the right part of the peak of the shifted spectrum covers the region around 1.056 eV (at 1200-1500 K), where the wide resolved resonance of Pu²⁴⁰ is located.

Table 7: Moderator Temperature Reactivity Coefficients (MTRC)

Temperature range (K)	K_{eff}^1	Std desv.	K_{eff}^2	Std desv.	MTRC pcm/K	
300 - 600	0.91465	0.0006	0.90500	0.00062	-3.89	± 0.49
600 - 800	0.90500	0.00062	0.98170	0.00061	-8.24	± 0.76
800 - 1200	0.89170	0.00061	0.88143	0.00060	-3.27	± 0.38
1200 - 1600	0.88143	0.00060	0.85662	0.00058	-8.21	± 0.39
1600 - 2000	0.85662	0.00058	0.82606	0.00058	-10.80	± 0.41

5 CONCLUSIONS

The present work is based on the pre-conceptual PBT and TADSEA designs and it focuses on the comparison of the behavior of several deep burn in-core fuel management strategies for LWR waste.

We analyzed the fuel cycle on TADSEA device based on driven and transmutation fuel that was proposed before for the General Atomic design of a gas turbine-modular helium reactor. We compared the spent fuel management strategies from LWR waste in PBT system called SF, DF and $DF + TF$, taking in count the decreasing of mass of Plutonium isotopes and Minor Actinides in relation to the initial load one, and decreasing of time evolution radiotoxicity of fuel discharge.

The results of burning for SF and DF strategies in PBT and TADSEA at stationary stage lead to a similar reduction of mass of Np^{237} , Pu^{239} y el Pu^{240} , to a less increase for DF of mass of Cm^{242} , Cm^{244} , Am^{243} y Pu^{242} , and how unfavorable effects a lightly increase of Am^{241} for DF (it is obtained for SF a significantly decrease) and a less decrease of Pu^{241} . The time evolution of radiotoxicity to discharge for both is the same.

The spent fuel management strategy called $DF + TF$ need a two step fuel cycle, but it achieves a similar decrease of mass of Am^{241} like SF, a decrease of mass of Am^{243} in a 66% (grow for SF) and a less increase of Cm^{244} , but mass of Pu^{238} increases. After 300 years radiotoxicity of discharge of $DF + TF$ strategy is 30 or 40% less than SF strategy.

But if we take account the poor energetic contribution of TF layer and it need a second step in reprocessing process, is necessary to make a careful evaluation of the alternative of burning MA in a fast system with full recycle, and using the spent fuel management strategy called DF to obtain the main goal, the extended destruction of Pu^{239} .

In this paper we calculated too the fuel and moderator reactivity temperature coefficients for the beginning of the first cycle for DF in PBT system. We obtained a very good agreement with those obtained before for AHTR using Plutonium fuel.

ACKNOWLEDGEMENTS

One of the authors (C García) thanks to Universidad Politécnia de Valencia for the support received from its INNOVA programme to finance his stay at the IIE to complete this study.

References

- [1] A. Abádanés, A. Pérez-Navarro, “*Engineering design studies for transmutation of nuclear waste with a gas-cooled pebble-bed ADS*”, ***Nuclear Engineering and Design***. **237**, **325**, **2007**.
- [2] The European technical working group on ADS , “*A European roadmap for developing Accelerator Driven Systems for nuclear waste incineration*”, **April 2001**.
- [3] C. García A. Pérez-Navarro, A. Escrivá, A. Abánades, Rosales J., L. García, “*Autonomous Hydrogen Generator Based on an ADS Transmutation System*”, **Paper sent to publish. 2009**.
- [4] Gregg McKinney et al., “*MCNPX 2.6x features (2006-2007)*”, **LA-UR-07-2053. Los Alamos National Laboratory 2007**.
- [5] LA-CP-05-0369, “*MCNPX Users Manual*”, **Version 2.5.0, April 2005**.
- [6] R.E.,Prael,H.,Lichtenstein, “*Use guide to LCS: The LAHET Code System*”, **Group X-6. MSB226. Los Alamos National Laboratory. (1989)**
- [7] C. Rodríguez, A Baxter, D.McEachern, M. Fikani, F. Venneri , “*Deep-Burn: making nuclear waste transmutation practical.*”, ***Nuclear Engineering and Desing***. **222 (2003) 299-317**.
- [8] Alberto. Tálamo, Waclaw Gudowski, Francesco Venneri, “*The burnup capabilities of the Deep Burn Modular Helium Reactor analyzed by the Monte Carlo Continuous Energy Code MCB*”, ***Annals of Nuclear Energy*** **31 (2004) 173-196**.
- [9] Jitka Zakova, Alberto Talamo , “*Analysis of reactivity coefficients of advanced high-temperature for plutonium and uranium fuels*”, ***Annals of Nuclear Energy*** **35. (2008) 904-916**.